Modern Physics Letters B, Vol. 8, No. 4 (1994) 239–246

ON THE MONTE CARLO SIMULATION APPROACH TO FOKKER–PLANCK EQUATIONS IN QUANTUM OPTICS

G. M. D'ARIANO and C. MACCHIAVELLO
Dipartimento di Fisica 'Alessandro Volta', Università degli Studi di Pavia via A. Bassi 6, I-27100 Pavia, Italy

S. MORONI
Scuola Internazionale Studi Superiori Avanzati, Strada Costiera 11, 134014 Trieste, Italy

Received October 1993

The suitability of the Monte Carlo simulation approach to Fokker–Planck equations in quantum optics is investigated. The method is especially useful for multimode analysis, and hence for studying realistic models of nonlinear optical systems. Here it is illustrated on the basis of two simple examples of application: i) a one-dimensional Fokker–Planck equation in the number representation, which describes a simple model of optical amplifier, and ii) the Van der Pol two-dimensional equation in the P-function representation.

Simulation methods have been recently introduced in quantum optics and proved to be very efficient for treating complex nonlinear systems. In Refs. 2 a Monte Carlo wave function method has been developed which allows the solution of the master equation. The master equation approach, however, is not suited to large numbers of photons, due to the high effective dimension of the truncated Hilbert space. This prevents its use in several situations of practical interest, for example, when studying lasers or optical amplifiers.

Apart from the case of very small numbers of photons, the Fokker–Planck equation is a more suitable tool for numerical evaluations. The general form of the Fokker–Planck equation is

$$\partial_t P(x, t) = -\nabla_x \cdot [Q(x, t)P(x, t)] + \frac{1}{2} \nabla_x \nabla_x : [D(x, t)P(x, t)], \qquad (1)$$

where $P(x, t)$ is a probability (or quasiprobability) distribution in the d-dimensional space of the vectors $x \in R^d$, $Q(x)$ is the drift vector, and $D(x)$ is the diffusion matrix. Depending on the analytical form of the drift and diffusion terms, Eq. (1) can model a wide class of phenomenology in quantum optics, also allowing a precise treatment of the noise of quantum origin in the presence of saturation and, more generally, nonlinear effects.[3] The vector x can represent a set of photon numbers for different modes of radiation, or a set of real and imaginary parts of complex field

amplitudes: the former case corresponds to a number representation probability distribution, the latter to a Wigner function quasiprobability (in this case we only consider initial conditions and diffusion matrices such that P will remain positive at all times).

Despite that the Monte Carlo simulation has been devised as a convenient tool for solving equations of the Fokker–Planck form,[1] it is yet largely unknown by researchers in quantum optics. In this paper we illustrate the method and its effectiveness in modeling quantum optical systems on the basis of some typical examples. We show that the simulation gives reasonably accurate estimates of several quantities of physical interest with a moderate computational effort. The algorithm is very simple to implement and to use, and can be readily applied to a wide range of complex models in quantum optics. As in the case of any statistical integration method, the present approach is particularly efficient when a multidimensional integral (i.e. a multimode analysis) is concerned and direct integration algorithms become prohibitive.

We now briefly outline the procedure, using a Green function formalism. Let us describe the probability $P(x, t)$ for a generic time t by means of a statistical ensemble of N configurations $\{x_1(t), x_2(t), \ldots, x_N(t)\}$. For $t = 0$, the ensemble is sampled from a given initial probability distribution $P(x, 0)$ by standard Metropolis algorithms.[4] The time evolution of the probability distribution is

$$P(x, t + \Delta t) = \int_{R^d} dx' G(x, x'; \Delta t) P(x', t) . \tag{2}$$

The Green function $G(x, x'; t)$, which acts as a transition probability for $P(x, t)$, is the solution of Eq. (1) with the initial condition $G(x, x'; 0) = \delta(x - x')$. A short time approximation, correct to second order in Δt, is

$$G(x, x'; \Delta t) = [\det D(2\pi\Delta t)^d]^{-1/2} \times \exp[-(x' - x + Q\Delta t) \cdot (2\Delta t D)^{-1} \cdot (x' - x + Q\Delta t)] . \tag{3}$$

The time evolution is simulated[8] by moving the configurations $\{x_1(t), x_2(t), \ldots, x_N(t)\}$ according to the distribution represented by the approximate Green function of Eq. (3):

$$x_i(t + \Delta t) = x_i(t) + Q[x_i(t)]\Delta t + E[x_i(t)] , \tag{4}$$

where E is a zero average Gaussian random variable with variance $D[x_i(t)]\Delta t$.

The value of a generic physical quantity is given by an average over the probability distribution of the relative function $F(x, t)$. We denote this average by $\langle\ \rangle$:

$$\langle F(t) \rangle \equiv \int F(x) P(x, t) dx . \tag{5}$$

The corresponding estimate given by the simulation, which we denote by $\bar{F}$, is obtained by averaging over the ensemble:

$$\overline{F(t)} \equiv \frac{1}{N} \sum_{i=1}^{N} F[x_i(t)] . \tag{6}$$

The central limit theorem ensures that the two averages (5) and (6) coincide in the limit $N \to \infty$. Due to the finite size N of the sample, $\overline{F(t)}$ has a statistical uncertainty whose estimate is

$$\overline{\Delta F(t)} \simeq \sqrt{\frac{\sigma_F^2(t)}{N}} = \sqrt{\frac{\overline{F(t)^2} - \overline{F(t)}^2}{N}} , \tag{7}$$

if the configurations are independent. The statistical error defined in Eq. (7) is a decreasing function of N, whereas the variance σ_F^2 is usually only weakly dependent on the dimension d of the configuration space. This should be compared with the number of steps needed for convergence of customary integration algorithms, which is an exponentially increasing function of the dimension d. For the calculations presented in this paper, in order to obtain reasonable estimated error bars, it was sufficient to consider $N \sim 10^4$–10^5.

The use of a finite time step Δt introduces a systematic bias in the computed averages, because the Green function of Eq. (3) is exact only in the limit of vanishing time step. In the practical calculation one can tune Δt short enough to produce a bias smaller than the statistical error in the measured quantities. For very accurate estimates, one should perform simulations with different time steps and extrapolate the results to $\Delta t \to 0$ (typically, both the statistical error and the systematic time step bias get larger for increasing order of the evaluated distribution moment). In the following we give two examples of application of the above method.

A. *A one-dimensional example*

In this first example we consider the Fokker–Planck equation which can be derived from the laser one-mode master equation of Ref. 5 in the limit of large photon saturation numbers. The probability distribution $P(\nu, \tau)$ describes the evolution of the normalized photon number $\nu = n/n_*$ for saturation number n_*, τ being the time rescaled by the cavity damping time. The drift and diffusion coefficients have the simple form

$$\begin{aligned} Q(\nu) = {} & (\nu + n_*^{-1})[n_{\text{th}} + \theta(1 + \nu + n_*^{-1})^{-1}] \\ & - \nu[1 + n_{\text{th}} + \theta'(1 + \nu)^{-1}] , \end{aligned} \tag{8}$$

$$\begin{aligned} D(\nu) = {} & \frac{1}{2n_*} \{(\nu + n_*^{-1})[n_{\text{th}} + \theta(1 + \nu + n_*^{-1})^{-1}] \\ & + \nu[1 + n_{\text{th}} + \theta'(1 + \nu)^{-1}]\} , \end{aligned} \tag{9}$$

where $n_{\rm th}$ is the thermal photon number, and θ and θ' are pumping parameters which are proportional to the injection rates of atoms in the excited and the ground state, respectively. The present simple model is also suited for describing a traveling wave optical amplifier or, equivalently, an active fiber amplifier for negligible depletion of the pumping radiation mode. The boundary condition $\nu \geq 0$ was imposed in the simulation by a reflecting barrier. A sample of the probability evolution is given in Fig. 1, where the function $P(\nu, \tau)$ is plotted for an input coherent state at three different values of τ.

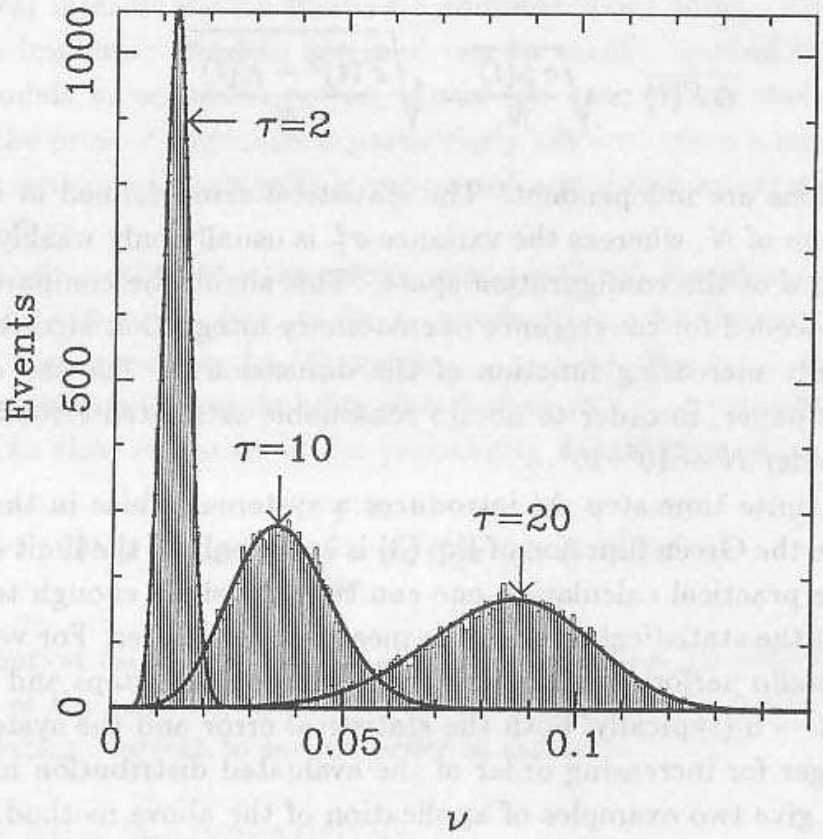

Fig. 1. Histograms representing the evolution of the probability distribution at $\tau = 2$, 10, and 20 for the one-dimensional Fokker–Planck equation with drift and diffusion coefficients given in Eqs. (8) and (9). Here $n_* = 10^4$, $\theta = 1.15$, and $n_{\rm th} = \theta' = 0$. At $\tau = 0$ an input coherent state has been used with $\langle n \rangle_0 = 100$. The full line represents the result from direct numerical integration.

As an application to a real system, we consider the traveling wave optical amplifier of Ref. 6. We evaluate the gain G and noise figure R defined as follows:

$$G = \frac{S_{\rm out}}{S_{\rm in}}, \qquad R = \frac{(S/R)_{\rm in}}{(S/R)_{\rm out}}. \tag{10}$$

In Eq. (10) $S_{\rm in}$ denotes the input mean photon number, whereas for on-off modulation, the output signal $S_{\rm out}$ is the difference between the output mean values in the presence and absence of input, namely, after subtraction of the amplified spontaneous emission (the signal-to-noise ratio $(S/R) = \langle n \rangle^2 / \langle \Delta n^2 \rangle$ contains the

number fluctuations $\langle \Delta n^2 \rangle$ averaged on equal on-off probabilities). In Fig. 2 the gain G and noise figure R obtained from a numerical simulation are plotted. These results can be compared with those reported in Ref. 6 (where, however, the amplified spontaneous emission has not been subtracted, leading to unphysical minimum noise figures lower than unit).

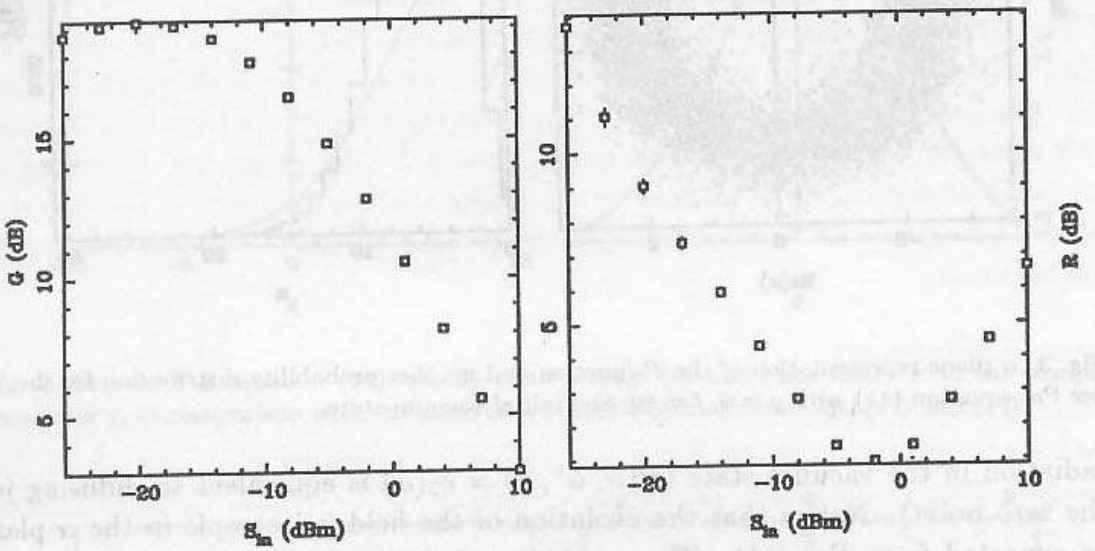

Fig. 2. Gain G and noise figure R for the traveling wave optical amplifier of Ref. 6, as a function of the input average signal in dBm units ($S_{\rm in}(\mathrm{dBm}) = 10\log(10^3 S_{\rm in})$).

B. *A two-dimensional example*

As a two-dimensional example, we consider the rotating Van der Pol oscillator, a popular simple model for the laser threshold.[7] The Fokker–Planck equation now describes the evolution of the quasiprobability P-function $P(\alpha, \alpha^*, t)$ in the interaction picture:

$$\frac{\partial}{\partial t} P(\alpha, \alpha^*, t) = \left\{ -\frac{\partial}{\partial \alpha}[(g - |\alpha|^2)\alpha] - \frac{\partial}{\partial \alpha^*}[(g - |\alpha|^2)\alpha^*] + 4\frac{\partial^2}{\partial \alpha \partial \alpha^*} \right\} P(\alpha, \alpha^*, t) . \tag{11}$$

In Eq. (11) the complex field amplitude α and the time t have been rescaled in order to have only the free parameter g (g is a pumping parameter, $g = 0$ corresponds to the threshold). As the diffusion matrix is constant positive, for initial $P(\alpha, \alpha^*, 0) \geq 0$ (for example, a coherent state, i.e. a delta-like P) the probability distribution remains positive for all times.

In Fig. 3 a sample of the probability distribution in the α plane along with the respective number probability distribution are given for fixed g and t, starting from

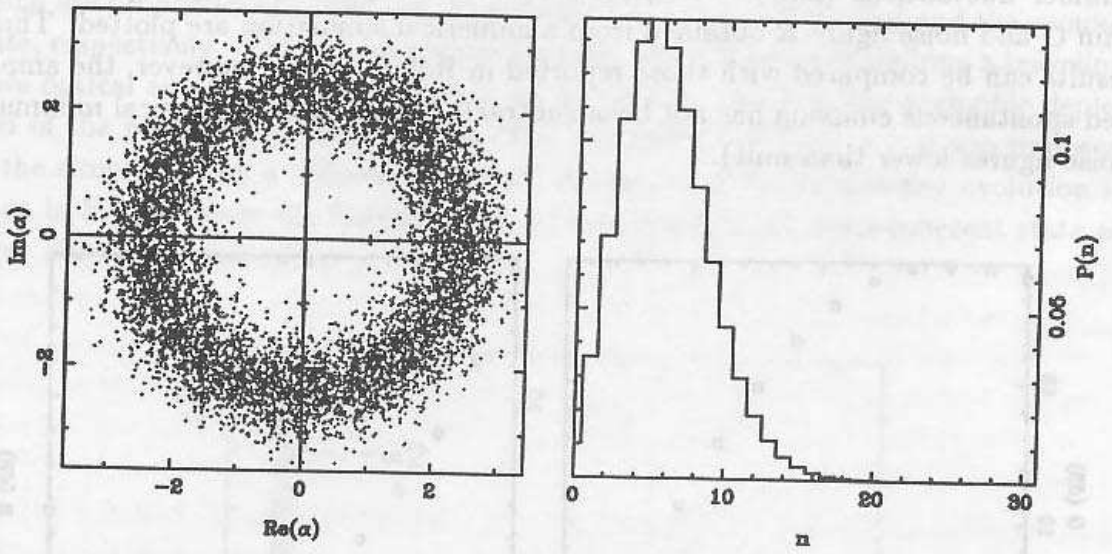

Fig. 3. α plane representation of the P-function and number probability distribution for the Van der Pol equation (11) with $g = 6$, $t = 10$, and initial vacuum state.

radiation in the vacuum state ($P(\alpha, \alpha^*, 0) = \delta_2(\alpha)$ is equivalent to diffusing just the zero point). Notice that the evolution of the field is isotropic in the α plane, as expected from Eq. (11). The number probability distribution is conveniently obtained, taking advantage of fast Fourier transform techniques, according to the following identity:

$$p(n, t) = \int_{-\pi}^{+\pi} \frac{dx}{2\pi} e^{-inx} \int d^2\alpha P(\alpha, \alpha^*, t) e^{|\alpha|^2(e^{ix}-1)} . \tag{12}$$

As a test of the method, in Fig. 4 the simulation steady state result for both the average $\langle n \rangle$ and the Fano factor $F = \langle \Delta n^2 \rangle / \langle n \rangle$ is compared with the analytical result which follows from the normal-ordered moments

$$\langle n \rangle = g + \frac{2}{\sqrt{\pi}} \frac{\exp(-g^2/4)}{1 + \mathrm{erf}(g/2)} , \tag{13}$$

$$\langle a^{\dagger 2} a^2 \rangle = g^2 + 2 + g \frac{2}{\sqrt{\pi}} \frac{\exp(-g^2/4)}{1 + \mathrm{erf}(g/2)} , \tag{14}$$

and the moments are evaluated according to

$$\langle a^{\dagger m} a^n \rangle \equiv \int d^2\alpha P(\alpha, \alpha^*) \alpha^{*m} \alpha^n . \tag{15}$$

The stationary results have been obtained upon evolving only one configuration for large number of steps ($N \sim 10^6$), taking advantage of the ergodic behavior of the solution.

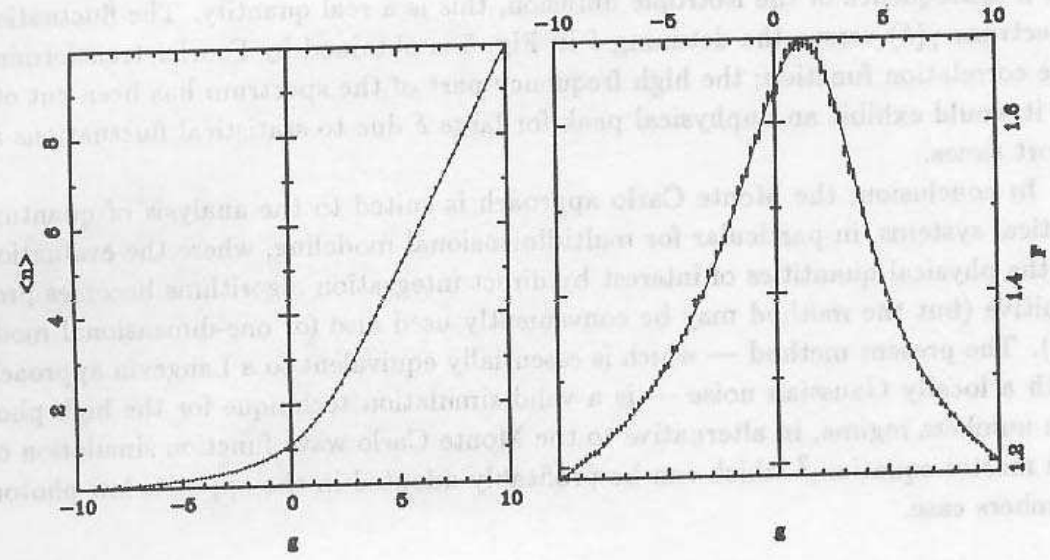

Fig. 4. Van der Pol equation (11): steady state average $\langle n \rangle$ and Fano factor F vs the pumping parameter g, in comparison with the analytical results obtained from Eqs. (13) and (14).

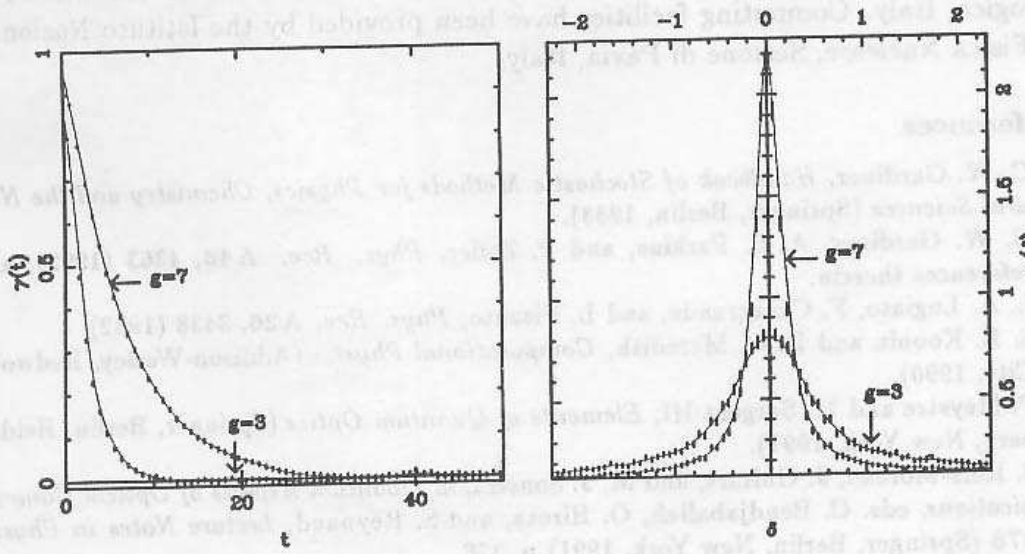

Fig. 5. Field correlation function $\gamma(t)$ and corresponding fluctuation spectrum $\gamma(\delta)$ vs detuning δ for $g = 3$ and 7 (the same model as in Fig. 4). The full lines are fits of the simulation points.

Finally, in Fig. 5 the field fluctuations after the steady state has been reached at $t = t_s$ are plotted for two different values of g. The field correlation function $\gamma(t)$ is given by

$$\gamma(t) \equiv \frac{\langle a^\dagger(t+t_s)a(t_s)\rangle}{\langle n(t_s)\rangle} = \frac{1}{\langle n(t_s)\rangle}\sum_{i=1}^{N} \alpha_i^*(t+t_s)\alpha_i(t_s)\,. \tag{16}$$

As a consequence of the isotropic diffusion, this is a real quantity. The fluctuation spectrum $\gamma(\delta)$ versus the detuning δ in Fig. 5 is obtained by Fourier transforming the correlation function; the high frequency part of the spectrum has been cut off, as it would exhibit an unphysical peak for large δ due to statistical fluctuations at short times.

In conclusion, the Monte Carlo approach is suited to the analysis of quantum optical systems, in particular for multidimensional modeling, where the evaluation of the physical quantities of interest by direct integration algorithms becomes prohibitive (but the method may be conveniently used also for one-dimensional models). The present method — which is essentially equivalent to a Langevin approach with a locally Gaussian noise — is a valid simulation technique for the high photon numbers regime, in alternative to the Monte Carlo wave function simulation of the master equation,[2] which can be profitably adopted in the opposite low photon numbers case.

Acknowledgements

We acknowledge L. Lugiato for discussions which stimulated this work. This work has been supported by the Ministero dell'Università e della Ricerca Scientifica e Tecnologica, Italy. Computing facilities have been provided by the Istituto Nazionale di Fisica Nucleare, Sezione di Pavia, Italy.

References

1. C. W. Gardiner, *Handbook of Stochastic Methods for Physics, Chemistry and the Natural Sciences* (Springer, Berlin, 1983).
2. C. W. Gardiner, A. S. Parkins, and P. Zoller, *Phys. Rev.* **A46**, 4363 (1992), and references therein.
3. L. A. Lugiato, F. Casagrande, and L. Pizzuto, *Phys. Rev.* **A26**, 3438 (1982).
4. S. E. Koonin and D. C. Meredith, *Computational Physics* (Addison-Wesley, Redwood City, 1990).
5. P. Meystre and M. Sargent III, *Elements of Quantum Optics* (Springer, Berlin, Heidelberg, New York, 1991).
6. S. Ruiz-Moreno, J. Guitart, and M. J. Soneira, in *Quantum Aspects of Optical Communications*, eds. C. Bendjaballah, O. Hirota, and S. Reynaud, *Lecture Notes in Physics* **378** (Springer, Berlin, New York, 1991) p. 376.
7. W. H. Louisell, *Quantum Statistical Properties of Radiation, Series in Pure and Applied Optics* (Wiley, New York, London, Sydney, Toronto, 1973).
8. H. Risken, *The Fokker–Planck Equation* (Springer, Berlin, 1989).